Int. J. Solids Structures, 1970, Vol. 6, pp. 661 to 675. Pergamon Press. Printed in Great Britain

LIMIT ANALYSIS WITH MULTIPLE LOAD PARAMETERS†

PHILIP G. HODGE, JR.‡

Illinois Institute of Technology, Chicago, Illinois, U.S.A.

Abstract—Upper and lower bound theorems are established for the yield-point interaction curve of a structure with more than one independently prescribed load parameter. The problem of finding the safety factor on the surface loading for a structure subject to a fixed body force is considered as a special case. The theory is illustrated with applications to beams and circular plates.

1. INTRODUCTION

THE PROBLEM of classical limit analysis may be stated as follows: given a rigid/plastic structure R subject to a prescribed set of loads $\mathbf{T}$ on a part B_T of the boundary of R, constrained against motion on the remainder B_V of the boundary, and with zero body forces, find the multiplier ρ such that the loads $\rho\mathbf{T}$ will just cause plastic deformation of the structure. The well known theorems of limit analysis prove that ρ is unique and provide methods for finding upper and lower bounds on ρ.

The restriction to zero body force is not often emphasized, but it is essential to the proofs of the theorems. To see this fact, let us consider the case where the body force distribution $\mathbf{F}$ is known and fixed (such as the weight of the structure), and it is desired to find the safety factor on the surface load $\mathbf{T}$ (such as a wind load).

The standard proof of the lower bound theorem begins by defining a statically admissible field as any state of stress σ_{ij}^0 which satisfies the yield condition and is in internal and external equilibrium with loads $\rho^0 T_i$. Therefore

$$\begin{aligned} \sigma_{ji,j}^0 + F_i &= 0 \quad \text{in} \quad R \\ \sigma_{ji}^0 n_i &= \rho^0 T_i \quad \text{on} \quad B_T. \end{aligned} \tag{1.1}$$

Let v_i and σ_{ji} be actual velocity and stress fields for plastic deformation and apply the principle of virtual work to both stress fields and the actual velocity field:

$$\begin{aligned} \int_R \sigma_{ij}\dot{\varepsilon}_{ij} &= \int_R F_i v_i + \rho \int_{B_T} T_i v_i \\ \int_R \sigma_{ij}^0\dot{\varepsilon}_{ij} &= \int_R F_i v_i + \rho^0 \int_{B_T} T_i v_i \end{aligned} \tag{1.2}$$

where

$$\dot{\varepsilon}_{ij} = \tfrac{1}{2}(v_{i,j} + v_{j,i}) \tag{1.3}$$

† This research was sponsored by the U.S. Office of Naval Research (DOMIIT Summary Report 1-41).
‡ Professor of Mechanics.

is the strain-rate field. Taking the difference between the two equations (1.2), we obtain

$$(\rho-\rho^0)\int_{B_T} T_i v_i = \int_R (\sigma_{ij}-\sigma_{ij}^0)\dot{\varepsilon}_{ij} \geq 0 \tag{1.4}$$

where the last step follows from Drucker's postulate [1] for a stable material:

$$(\sigma_{ij}-\sigma_{ij}^0)\dot{\varepsilon}_{ij} \geq 0. \tag{1.5}$$

Now, if there were no body forces, it would follow from thermodynamics that since $\rho\int_{B_T} T_i v_i$ represented all of the external rate of work of a real plastic deformation, the strict inequality

$$\rho\int_{B_T} T_i v_i > 0 \tag{1.6}$$

would be satisfied. Therefore, since ρ is positive (1.4) would lead to the desired conclusion

$$\rho^0 \leq \rho. \tag{1.7}$$

However, although the body force does not appear in (1.4) explicitly, its presence in the problem means that (1.6) must be replaced by

$$\int_V F_i v_i + \rho\int_{B_T} T_i v_i > 0. \tag{1.8}$$

Therefore, no conclusion can be drawn concerning the sign of the integral in (1.4), and hence (1.7) may be either true or false.

Consider next a different problem associated with the same situation in which ρ is to be the safety factor for *all* loads **F** and **T**. In this case (1.4) is replaced by

$$(\rho-\rho^0)\left(\int_v F_i v_i + \int_{B_T} T_i v_i\right) \geq 0 \tag{1.9}$$

and (1.8) by

$$\rho\left(\int_v F_i v_i + \int_{B_T} T_i v_i\right) > 0. \tag{1.10}$$

Therefore, in this case (1.7) is always valid.

A more general problem, which includes both of the above as special cases is one where we wish to prescribe safety factors on both the body force and the surface loads, with the two factors not necessarily equal. Thus, we are concerned with pairs of numbers ρ_1, ρ_2 such that the loads $\rho_1\mathbf{T}$ on the surface and $\rho_2\mathbf{F}$ in the interior just cause plastic deformation. In geometric terms, we seek a certain domain in a load space with coordinates ρ_1 and ρ_2. It turns out that this domain is a convex curve with the further property that when the vector $\boldsymbol{\rho} = (\rho_1, \rho_2)$ is inside the curve no plastic deformation occurs, whereas when it is outside the curve no equilibrium state exists for a perfectly plastic material.

The above problem is, in turn, a special case of a structure subjected to any number of independently prescribed loads which was considered in [2]. In the next section we shall develop the theory in terms of that more general problem and we shall extend the results to include an explicit proof of two generalized limit analysis theorems.

The significance of the theorems is illustrated in Section 3 by application to the simple case of a cantilever beam subject to its own weight and to an end load. Then, as a less trivial example, we consider a circular plate pierced by a central tube and subject to pressure and to a shear force due to the tube.

2. THEORY

Let R be a given structure with boundary B, and let Q_α, $\dot{q}_\alpha$ ($\alpha = 1, \ldots, r$) be appropriate generalized stresses and strain rates for R [3]. Let R be subject to m independently prescribed generalized surface traction distributions $\mathbf{T}_k(\mathbf{x})$, to n–m generalized body force distributions $\mathbf{F}_k(\mathbf{x})$ and, possibly, to zero velocity constraints. We note that the domains on B of $\mathbf{T}_k$ and $\mathbf{T}_l$ may coincide, intersect, or be disjoint. It is, of course, assumed that the total prescription of traction and velocity is consistent with a well-posed boundary value problem.

We allow each independent force to be multiplied by a parameter ρ_k, and consider the structure under the total loading

$$\begin{aligned} \mathbf{T}(\mathbf{x}, \boldsymbol{\rho}) &= \sum_{1}^{m} \rho_k \mathbf{T}_k(\mathbf{x}) \qquad \mathbf{x} \text{ on } B \\ \mathbf{F}(\mathbf{x}, \boldsymbol{\rho}) &= \sum_{m+1}^{n} \rho_k \mathbf{F}_k(\mathbf{x}) \qquad \mathbf{x} \text{ on } R. \end{aligned} \tag{2.1}$$

We define a *statically admissible stress state* as a generalized stress distribution Q_α^0 and a *load vector* $\boldsymbol{\rho}^0$ such that Q_α^0 satisfies the yield condition and is in equilibrium with loads defined by (2.1) with $\boldsymbol{\rho}$ replaced by $\boldsymbol{\rho}^0$.

To define a *kinematically admissible state* we begin with any generalized velocity fields $\mathbf{w}^*$ on B and $\mathbf{v}^*$ on R which satisfy continuity and boundary conditions. Next, a generalized strain-rate field $\dot{q}_\alpha^*$ is derived from $\mathbf{v}^*$ by the appropriate strain-rate–velocity relations, and a stress field Q_α^* is obtained from $\dot{q}_\alpha^*$ by the flow rule and yield condition. We then define the components of a *mode vector* $\mathbf{E}^*$ by

$$\begin{aligned} E_k^* &= \int_B \mathbf{T}_k \cdot \mathbf{w}^* \qquad k = 1, \ldots, m \\ E_k^* &= \int_R \mathbf{F}_k \cdot \mathbf{v}^* \qquad k = n+1, \ldots, n \end{aligned} \tag{2.2}$$

and require that $\mathbf{v}^*$ and $\mathbf{w}^*$ be such that $\mathbf{E}^* \neq 0$. Finally, a *kinematically admissible flat* $\mathfrak{F}$ is defined in load space as the locus of vectors $\boldsymbol{\rho}^*$ which satisfy

$$\boldsymbol{\rho}^* \cdot \mathbf{E}^* = \int_R Q_\alpha^* \dot{q}_\alpha^*. \tag{2.3}$$

Geometrically, $\boldsymbol{\rho}^*$ defines an $n-1$ dimensioned hyperplane which is perpendicular to the mode vector.

We can apply the principle of virtual work to any combination of statically and kinematically states to obtain

$$\begin{aligned}\int_R Q_\alpha^0 \dot{q}_\alpha^* &= \int_B \mathbf{T}\,.\,\mathbf{w}^* + \int_R \mathbf{F}\,.\,\mathbf{v}^* \\ &= \sum_1^m \rho_k^0 \int_B \mathbf{T}_k\,.\,\mathbf{w}^* + \sum_{m+1}^n \rho_k^0 \int_R \mathbf{F}_k\,.\,\mathbf{v}^*\end{aligned} \tag{2.4}$$

where we have used (2.1). Therefore, in view of (2.2),

$$\int_R Q_\alpha^0 \dot{q}_\alpha^* = \boldsymbol{\rho}^0\,.\,\mathbf{E}^*. \tag{2.5}$$

Next, we define a *yield-point state* Q_α, $\dot{q}_\alpha$, ρ, etc. as any state which is in equilibrium and which satisfies the flow rule with a non-trivial velocity field, i.e. such that the strict inequality

$$\boldsymbol{\rho}\,.\,\mathbf{E} > 0 \tag{2.6}$$

is satisfied. The set of points $\boldsymbol{\rho}$ which are part of a yield point state will form a certain locus in load space which we shall refer to as the *yield-point interaction surface*.

It is evident from our definitions that the yield-point state is both statically and kinematically admissible. Therefore, either or both of the states in (2.5) may be replaced by a yield-point state. Further, Drucker's stability postulate [1] may be applied to conclude

$$(Q_\alpha - Q_\alpha^0)\dot{q}_\alpha \geq 0 \tag{2.7}$$

$$(Q_\alpha^* - Q_\alpha)\dot{q}_\alpha^* \geq 0. \tag{2.8}$$

In terms of the preceding definitions the two generalized theorems of limit analysis are conveniently stated as follows in the geometrical terminology of load space.

Lower bound theorem

A statically admissible state can be associated with the load state $\boldsymbol{\rho}^0$ if and only if $\boldsymbol{\rho}^0$ is on or within the yield-point interaction surface.

Upper bound theorem

A kinematically admissible state can be associated with the load state ρ^* if and only if $\boldsymbol{\rho}^*$ is outside of or on the yield-point interaction surface.

To prove the lower bound theorem, we first integrate (2.7) over R and use (2.5) to obtain

$$(\boldsymbol{\rho} - \boldsymbol{\rho}^0)\,.\,\mathbf{E} \geq 0 \tag{2.9}$$

As was shown in [2], (2.9) implies that the interaction surface is convex and that $\mathbf{E}$ is an exterior normal to the surface at the point $\boldsymbol{\rho}$.

By definition, a load point on the interaction surface Γ is associated with a yield state and hence with a statically admissible state. For any other load point P, we can draw a ray (not unique, of course) which cuts the interaction surface in two points A and C, Fig. 1(a). Then

$$\boldsymbol{\rho}^0(P) = \boldsymbol{\rho}(A) + \lambda[\boldsymbol{\rho}(C) - \boldsymbol{\rho}(A)] \tag{2.10}$$

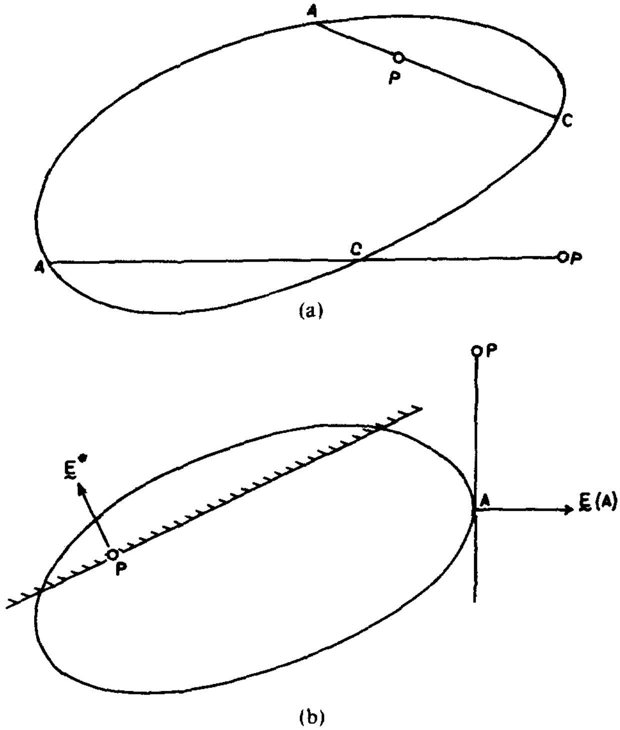

FIG. 1. Load space for proof of theorems.
(a) Lower bound theorem.
(b) Upper bound theorem.

where, in view of the convexity of Γ,

$$0 < \lambda < 1 \quad \text{for} \quad P \text{ inside } \Gamma \tag{2.11}$$

$$1 < \lambda \quad \text{for} \quad P \text{ outside } \Gamma. \tag{2.12}$$

For P inside Γ, we construct the stress state

$$Q_\alpha^0(P) = Q_\alpha(A) + \lambda[Q_\alpha(C) - Q_\alpha(A)]. \tag{2.13}$$

Since all equilibrium relations are linear, Q_α^0 is in equilibrium with the load vector $\boldsymbol{\rho}^0$ defined by (2.10); since $Q_\alpha(A)$ and $Q_\alpha(C)$ are on or within the yield curve of the material, and since this curve is convex [1], it follows from (2.11) that Q_α^0 satisfies the yield criterion. Therefore, (2.13) defines a statically admissible state for any point P inside Γ.

On the other hand, if any point P outside of Γ were statically admissible, we could take C and P as the yield-point and admissible states in (2.9) and use (2.10) to obtain

$$(1-\lambda)\{[\boldsymbol{\rho}(C) - \boldsymbol{\rho}(A)] \,.\, \mathbf{E}(C)\} \geq 0. \tag{2.14}$$

Since the yield-point state A is statically admissible, (2.9) shows that the brace in (2.14) is non-negative, and the non-uniqueness of the ray PCA can always be invoked to make it strictly positive. Therefore (2.14) requires

$$\lambda < 1. \tag{2.15}$$

The contradiction between (2.12) and (2.15) shows that P outside of Γ is not statically admissible and hence completes the proof.

To prove the upper bound theorem, we first integrate (2.8) over R and use the definition (2.3) to obtain

$$(\boldsymbol{\rho}^* - \boldsymbol{\rho}) \cdot \mathbf{E}^* \geq 0. \tag{2.16}$$

Let $\boldsymbol{\rho}(P)$ be the vector to a load point P which is on or outside of the interaction surface Γ and let $\mathfrak{F}$ be any hyperplane through P which is tangent to Γ; denote a point of tangency by A [Fig. 1(b)]. Since A is a yield-point state, it is kinematically admissible and we shall show that $\boldsymbol{\rho}(P)$ is a member of the kinematically admissible flat associated with the state A.

We first note that the definition of $\mathfrak{F}$ allows us to write

$$\boldsymbol{\rho}(P) = \boldsymbol{\rho}(A) + \boldsymbol{\xi} \tag{2.17}$$

where $\boldsymbol{\xi}$ is a vector in the hyperplane $\mathfrak{F}$. Then, since $\mathbf{E}(A)$ is normal to the interaction curve at A it is normal to $\mathfrak{F}$ and hence

$$\mathbf{E} \cdot \boldsymbol{\xi} = 0. \tag{2.18}$$

Finally, we apply (2.5) to the yield-point state A, and use (2.17) and (2.18) to obtain

$$\int_R Q_\alpha \dot{q}_\alpha = \boldsymbol{\rho}(A) \cdot \mathbf{E} = \boldsymbol{\rho}(P) \cdot \mathbf{E}. \tag{2.19}$$

Therefore, it follows from (2.3) that $\boldsymbol{\rho}(P)$ is on the kinematically admissible flat associated with A.

That P cannot be inside the interaction curve follows from the same arguments that show Γ is convex and $\mathbf{E}$ is normal to Γ. Indeed, if there exists an $\mathbf{E}^* \neq 0$ associated with P, (2.16) shows immediately that all yield-point states $\boldsymbol{\rho}$ must be on one side of the plane through P normal to E^*, Fig. 1(b). Therefore P cannot be in the interior of Γ and the contradiction completes the proof of the theorems.

3. BEAM EXAMPLE

Consider the cantilever beam in Fig. 2(a), where T and P are given positive numbers. We define dimensionless quantities by

$$\begin{aligned} m &= M/M_0 \qquad & x &= X/L \\ p &= PL^2/2M_0 \qquad & t &= TL/M_0 \end{aligned} \tag{3.1}$$

and consider the structure under loads $\boldsymbol{\rho}_1 t, \boldsymbol{\rho}_2 p$; without loss of generality we take $t = p = 1$. Then, for a statically admissible state, equilibrium demands

$$m^0(x) = -\rho_1^0 x - \rho_2^0 x^2 \tag{3.2}$$

and the yield requirement is

$$-1 \leq m^0(x) \leq 1 \quad \text{for all} \quad 0 \leq x \leq 1. \tag{3.3}$$

The constraints (3.3) must always apply at the root of the beam $x = 1$, hence

$$-1 \leq \rho_1^0 + \rho_2^0 \leq 1. \tag{3.4a, b}$$

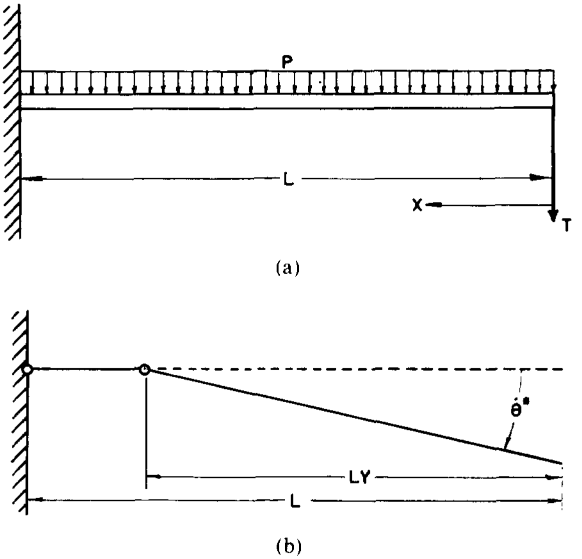

FIG. 2. Cantilever beam.
(a) Loaded beam.
(b) Mechanism.

In addition, if ρ_1^0 and ρ_2^0 are such that the extremum of the quadratic function (3.2) falls within the beam length, (3.3) must be satisfied at the extreme point. Thus

$$\text{if } 0 \le -\rho_1^0 \le 2\rho_2^0 \qquad \text{then} \quad \rho_2^0 \ge \tfrac{1}{4}(\rho_1^0)^2 \tag{3.4c}$$

$$\text{if } 0 \ge -\rho_1^0 \ge 2\rho_2^0 \qquad \text{then} \quad \rho_2^0 \le -\tfrac{1}{4}(\rho_1^0)^2. \tag{3.4d}$$

Figure 3 shows the boundary of the domain defined by (3.4).

To apply the upper bound theorem, consider the family of mechanisms defined by Fig. 2(b). The mode vector is easily obtained in the form

$$\mathbf{E}^* = M_0\dot{\theta}^*(y, y^2) \tag{3.5}$$

whereas it follows from (2.3) that

$$\boldsymbol{\rho}^* \,.\, \mathbf{E}^* = \int_{0^-}^{L^+} M^*\kappa^* = M_0|\dot{\theta}^*|. \tag{3.6}$$

Therefore, (2.16) shows that

$$\boldsymbol{\rho} \,.\, \mathbf{E}^* = M_0\dot{\theta}^*(\rho_1 y + \rho_2 y^2) \le M_0|\dot{\theta}^*|$$

or, equivalently

$$-1 \le \rho_1 y + \rho_2 y^2 \le 1. \tag{3.7}$$

For any choice of y, $0 \le y \le 1$, (3.7) can be used to draw a linear upper bound on the interaction curve as illustrated in Fig. 3. However, in this simple example one may choose y analytically to find the best upper bound. Indeed, it is evident that the restrictions are

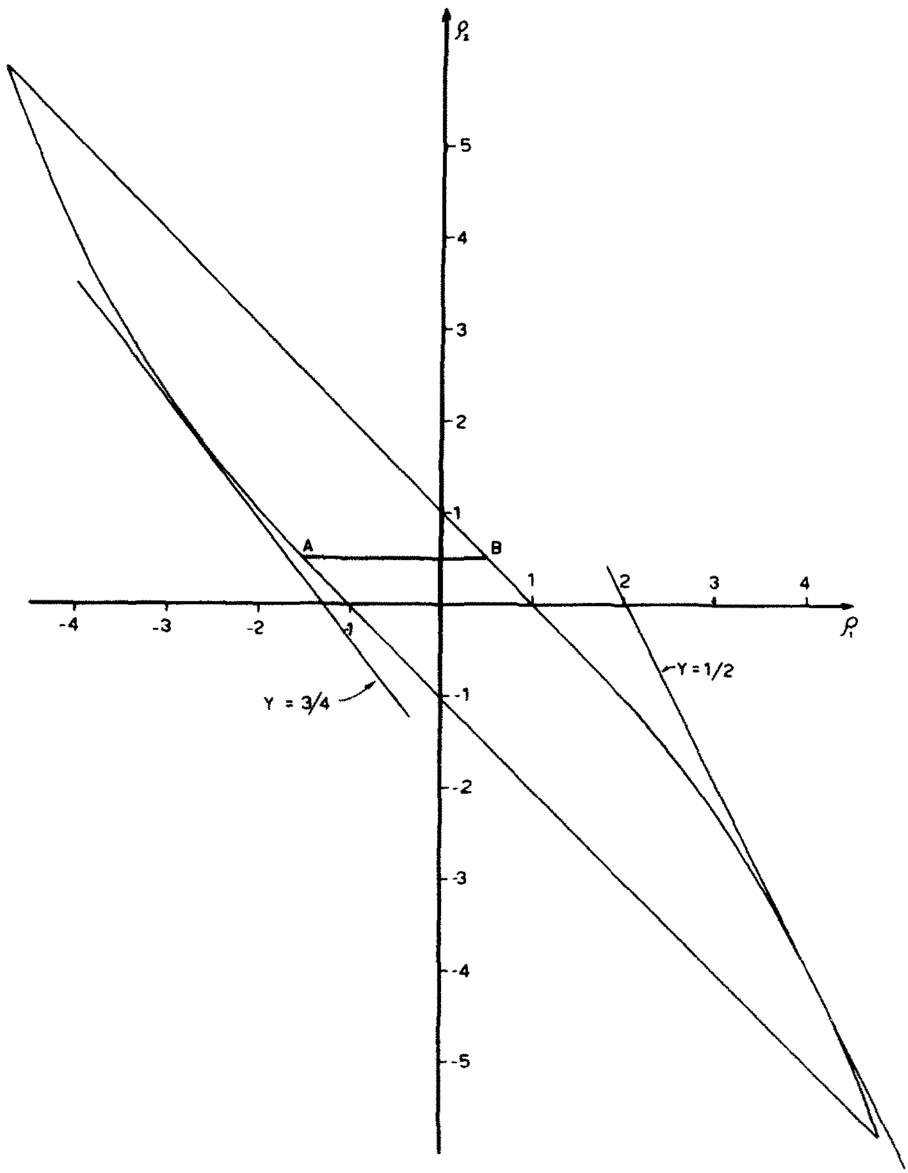

FIG. 3. Beam interaction curve.

exactly the same as (3.3) so that the upper and lower bounds coincide and we have found the exact interaction curve.

In terms of this example, we can now clarify the problem posed in the Introduction concerning fixed body force loads. If we have no body force, $\rho_2 = 0$, and, in view of the symmetry of Fig. 3, the yield-point behavior is fully prescribed by the single positive number $\rho_1 = \rho = 1$.

However, for any non-zero body force, we fix a non-zero value of ρ_2 as shown by line AB in Fig. 3 and it now requires *two* numbers to specify the yield-point behavior. Therefore, a single number ρ is not properly defined in this case and it is not surprising that we were unable to prove (1.7). If we do define two yield-point loads, say ρ^+ and ρ^-, then it is evident that any mechanism associated with ρ^+ will have

$$E_1 = \int_{B_T} T_i v_i > 0 \tag{3.8}$$

whereas for ρ^-, $E_1 < 0$. Therefore (1.4) shows that

$$\rho^- \leq \rho_0 \leq \rho^+ \tag{3.9}$$

which is a proper generalization of (1.7) and a proper special case of the lower bound theorem proved in the preceding section.

4. PLATE EXAMPLE

As a less trivial application, we consider an annular plate of inner and outer radii A and B, respectively (Fig. 4). The outer edge is welded to a fixed support and the inner edge is welded to a rigid pipe which transmits a shear force S per unit length to the plate. In addition, the plate is subjected to a pressure P per unit area. It is desired to determine the plastic interaction curve between P and S.

The rotationally symmetric plate problem is fully defined by a deflection rate W, the generalized strain-rates

$$K_r = -\mathrm{d}^2 W/\mathrm{d}R^2 \qquad K_\theta = -\mathrm{d}W/(R\,\mathrm{d}R)$$

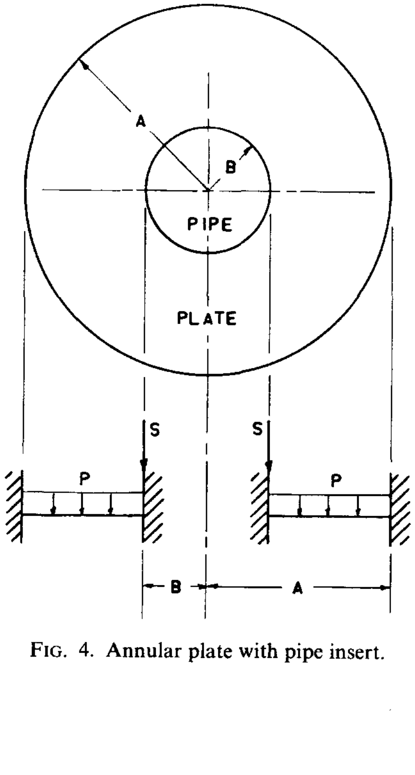

FIG. 4. Annular plate with pipe insert.

and the corresponding generalized stresses M_r and M_θ, all as functions of the radial distance R. We introduce the dimensionless quantities

$$\begin{array}{lll} r = R/A & b = B/A & w = W/A \\ m = M/M_0 & \kappa = AK & \mathbf{e} = \mathbf{E}/2\,AM_0 \\ p = PA^2/6M_0 & s = SB/M_0 & \end{array} \tag{4.1}$$

where M_0 is the fully plastic moment. We shall use primes to denote differentiation with respect to r. Without loss of generality we may set $p = s = 1$ and look for the interaction curve relating the loads $\rho_1 S$ and $\rho_2 P$.

A statically admissible moment state (m_r^0, m_θ^0) must satisfy the yield condition and equilibrium. We shall assume Tresca's yield condition (Fig. 5):

$$\max\,[|m_r^0|, |m_\theta^0|, |m_r^0 - m_\theta^0|] \leq 1. \tag{4.2a}$$

All equilibrium requirements, including the shear boundary condition at $r = b$ will be satisfied if m_r^0 is continuous and

$$(rm_r^0)' - m_\theta^0 = -\rho_1^0 - 3\rho_2^0(r^2 - b^2). \tag{4.2b}$$

A kinematically admissible state is defined by any continuous deflection rate w^* which satisfies the boundary condition

$$w^*(1) = 0 \tag{4.3a}$$

The mode vector (2.2) is given by

$$\mathbf{e}^* = \left[w^*(b), 6\int_b^1 w^*(r)r\,\mathrm{d}r \right]. \tag{4.3b}$$

The generalized strain-rate vector is

$$\dot{q}_\alpha^* \equiv (\kappa_r^*, \kappa_\theta^*) = [-(w^*)'', -(w^*)'/r] \tag{4.3c}$$

whence it follows from (2.3) that the associated kinematically admissible flat is defined by

$$\boldsymbol{\rho}^* \cdot \mathbf{e}^* = \int_b^1 (m_r^* \kappa_r^* + m_\theta^* \kappa_\theta^*) r\,\mathrm{d}r. \tag{4.3d}$$

The moment state in (4.3d) must be a point (m_r^*, m_r^*) on the yield hexagon of Fig. 5 such that

$$q_\alpha^* = \lambda^* n_\alpha^* \tag{4.3e}$$

where n_α^* is a unit outward normal to Fig. 5 at (m_r^*, m_θ^*), and $\lambda^* \geq 0$.

Any solution of (4.2) furnishes a $\boldsymbol{\rho}^0$ which is on or within the interaction curve. Any solution of (4.3) furnishes a ρ^* which is on or outside of the interaction curve. Finally, if all of (4.2) and (4.3) are satisfied, a complete solution will be defined, and the associated $\boldsymbol{\rho}$ must be precisely on the interaction curve.

For small values of b and some range for ρ_1, we might expect the complete solution to be associated with the stress profile BCD at yield [Fig. 5(a)] which was found by Hopkins and Prager [4] for a solid plate under uniform pressure. The moment solution according

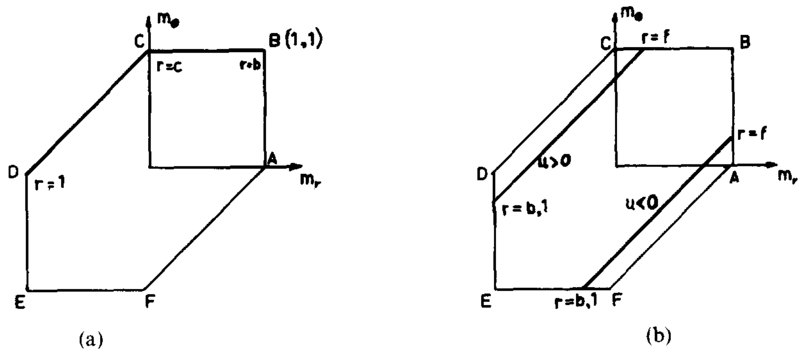

FIG. 5. Tresca yield condition.
(a) Profiles for complete solution.
(b) Profiles for lower bound.

to this hypothesis is

$$\begin{aligned} b \le r \le c: m_r &= 1-(\rho_1/r)(r-b)^2(r+2b)-(\rho_2/r)(r-b) \\ c \le r \le 1: m_r &= -1+\log r+\tfrac{3}{2}\rho_1(1+2b^2\log r-r^2)-\rho_2 \log r \end{aligned} \tag{4.4}$$

where ρ_1 and ρ_2 are given in terms of the parameter c by

$$\begin{aligned} \rho_1 &= [(c^3+2b^3)\log c+\tfrac{3}{2}c(1-c^2)-(c-b)^2(c+2b)]/d \\ \rho_2 &= (b\log c+c-b)/d \\ d &= (c-b)[(c^2+cb+b^2)\log c+\tfrac{3}{2}(1-c^2)]. \end{aligned} \tag{4.5}$$

Curve $CHABJ'C'$ in Fig. 6 shows the curve (4.5). Since the solution of this problem is obviously symmetric about the origin in load space, we have also drawn the reflection $C'H'A'B'JC$.

Now, the solution (4.4) and (4.5) satisfies equilibrium and the equations $m_\theta = 1$ or $m_\theta - m_r = 1$. However, we have not yet enforced the requirement that it lie on the finite portions of those lines as drawn in Fig. 5(a). A necessary and sufficient condition that this requirement be met is that $m_r' \le 0$ in all $b \le r \le 1$. This requirement is easily checked numerically by computing m_r' at $r = b$, $r = c$ and $r = 1$. The resulting statically admissible portion of (4.5) is shown as AB in Fig. 6. Using the reflected portion $A'B'$ and the fact that the interaction curve is convex, we have established the closed curve $ABA'B'$ as a lower bound.

A velocity field based on the profile of Fig. 5(a) and satisfying (4.3a) and (e) is

$$\begin{aligned} b \le r \le c: w &= C(1-\log c-r/c) \\ c \le r \le 1: w &= -C\log r \end{aligned} \tag{4.6}$$

and the associated mode vector is

$$\mathbf{e} = (1/c)[c-b-c\log c, (c-b)^2(c+2b)+(3/2)c(1-c^2)+3b^2c\log c]. \tag{4.7a}$$

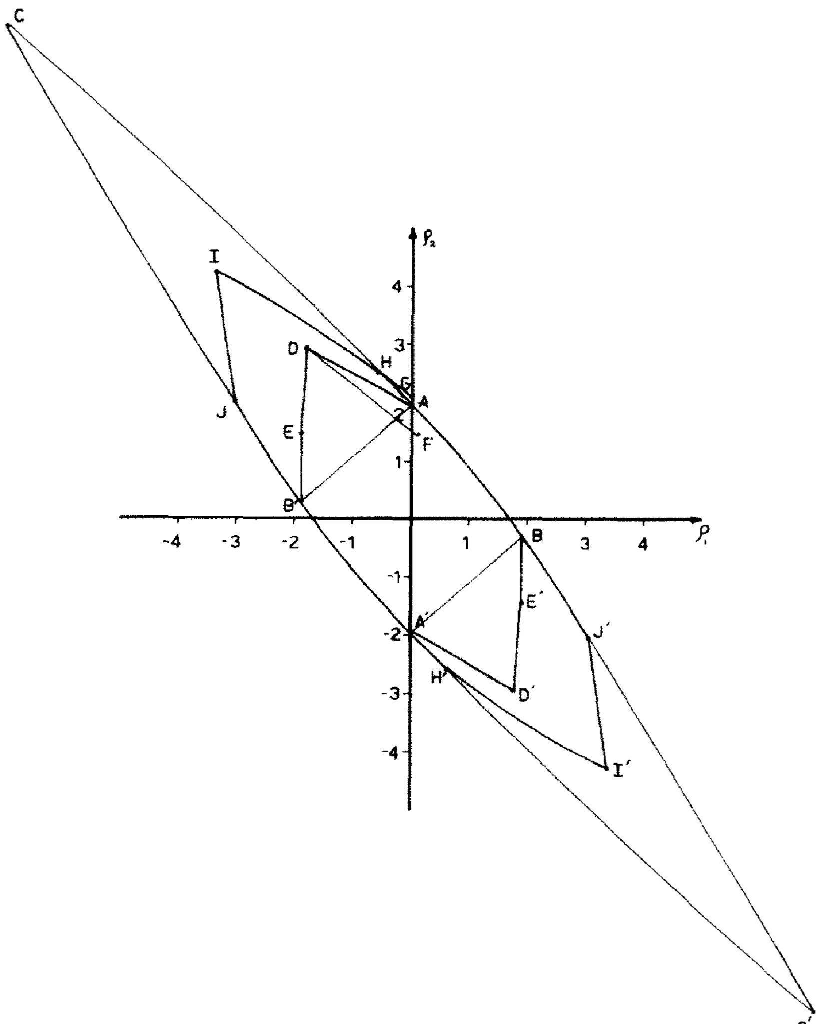

FIG. 6. Plate interaction curve, $b = 0{\cdot}1$.

In computing (4.3d) we note that w' does not satisfy the clamped condition at $r = b$ and $r = 1$, hence a finite contribution to the integral occurs at those two points. Thus

$$\begin{aligned} \boldsymbol{\rho} \cdot \mathbf{e} &= |bw'(b)| + \int_b^c (C/c)r\,\mathrm{d}r + \int_c^1 (C/r)\,\mathrm{d}r + |w'(1)| \\ &= C(2 - \log c) \end{aligned} \tag{4.7b}$$

where we have taken $C > 0$.

For any choice of c equations (4.7) define a straight line which is everywhere on or outside of the interaction curve:

$$\begin{aligned} g(c, \rho_1, \rho_2) \equiv\ & \rho_1(1 - \log c - b/c) - (2 - \log c) \\ & + \rho_2[3b^2 \log c + (-c^2 - 6b^2 + 3 - 4b^3/c)/2] = 0. \end{aligned} \tag{4.8}$$

Therefore, the envelope of (4.8) obtained by eliminating c between (4.8) and

$$\partial g/\partial c \equiv \rho_1(b-c)+\rho_2(3b^2c-c^3-2b^3)+c = 0 \tag{4.9}$$

will be an upper bound for the interaction curve. It is readily verified that equations (4.8) and (4.9) are equivalent to (4.5) so that the evelope is $CABC'$ in Fig. 6. Therefore, using symmetry with respect to the origin, we have constructed to upper bound $CABC'A'B'$. On the basis of the profile in Fig. 5(a), then, we have both upper and lower bounds for the entire range of ρ_1 and ρ_2, together with part of the exact solution.

Rather than seek to extend the exact solution, we look directly for some improved bounds. Let us consider a profile of the form

$$m_\theta^0 = m_r^0+u \tag{4.10}$$

where u is a constant. The solution of equation (4.2b) is evidently

$$m_r^0 = A-\tfrac{3}{2}\rho_2^0r^2+(3\rho_2^0b^2+u-\rho_1^0)\log r. \tag{4.11}$$

We take ρ_2^0 to be positive for definiteness, and define $r = f$ as the single root of $m_r' = 0$. Then

$$\rho_1^0 = u-3\rho_2^0(f^2-b^2) \tag{4.12}$$

and equation (4.11) can be rewritten in the form

$$m_r^0 = A-\tfrac{3}{2}\rho_2^0(f^2\log r^2-r^2). \tag{4.13}$$

We wish to eliminate the three parameters, A, f and u, in order to obtain a relation between ρ_1^0 and p_2^2. To this end we need four equations including (4.12). Now, with reference to Fig. 5(b), the stress point will move monotonically along one of the profiles as r increases from b to f, and will move in the reverse direction as r increases from f to 1. Therefore, a reasonable basis for obtaining the three additional equations is to require that the stress points corresponding to $r = b, f$, and 1 lie on the yield curve.

There are four possibilities depending upon the sign of u and whether $r = f$ is a minimum or maximum. It turns out that the case where m_r^0 is a maximum at f is of interest. Then for $u > 0$, the three equations are

$$\begin{aligned} m_r(b) &= A+\tfrac{3}{2}\rho_2^0(f^2\log b^2-b^2) = -1 \\ m_r(1) &= A-\tfrac{3}{2}\rho_2^0 \qquad\qquad\qquad = -1 \\ m_\theta(f) &= A+\tfrac{3}{2}\rho_2^0(f^2\log f^2-f^2)+u = 1. \end{aligned} \tag{4.14}$$

Three similar equations are obtained for $u < 0$. Elimination of A and solution for f leads to results which can be written

$$f = [(b^2-1)/\log b^2]^{\frac{1}{2}} \tag{4.15}$$

$$\rho_2^0 = \tfrac{2}{3}(2-|u|)(1-f^2+f^2\log f^2)^{-1}. \tag{4.16}$$

For a given hole radius b, f is determined by (4.15), and it is easily verified that $b \leq f \leq 1$. Equations (4.16) and (4.12) then give ρ_2^0 and ρ_1^0 as functions of the parameter u, subject to $0 \leq |u| \leq 1$. Since these functions are piecewise linear, the resulting curve will consist of linear segments in Fig. 6 connecting the points E, D and F corresponding respectively to $u = -1, 0$ and 1.

In view of the previous lower bound and the convexity of the interaction curve, DA is an improved lower bound over DF and EB' can be drawn as a lower bound. Finally, it follows from symmetry that the lower bound now stands as $ABE'D'A'BEDA$.

Improved upper bounds are obtained by considering the linear profiles shown in Fig. 7. According to Fig. 7(a),

$$\begin{aligned} b \leq r \leq c: w^* &= A(1-c) \\ c \leq r \leq 1: w^* &= A(1-r) \end{aligned} \tag{4.17}$$

$$\begin{aligned} \mathbf{e}^* &= A(1-c)[1, 1+c+c^2-3b^2] \\ \boldsymbol{\rho}^* . \mathbf{e}^* &= |cw^{*\prime}(c)| + |w^*(1) - w^*(c)| + |w^{*\prime}(1)| = 2|A|. \end{aligned} \tag{4.18}$$

If A is positive it follows from (4.18) that the straight line

$$\rho_1^* + \rho_2^*(1+c+c^2-3b^2) = 2/(1-c) \tag{4.19}$$

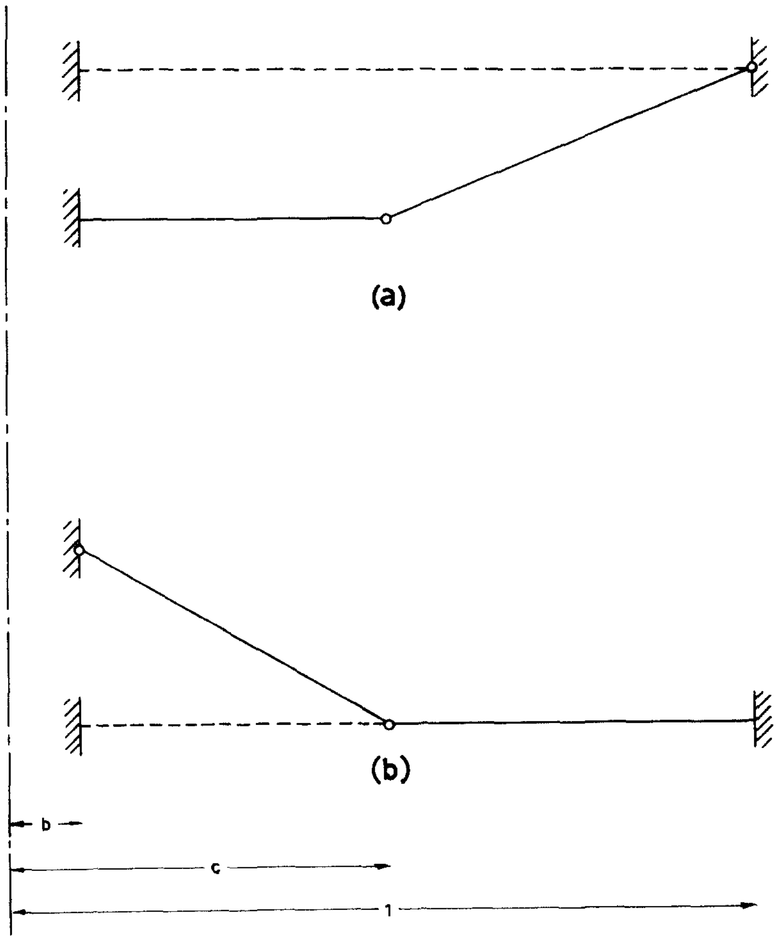

FIG. 7. Plate mechanisms.

is everywhere on or outside of the interaction curve for any choice of c. Therefore, the envelope of (4.19),

$$\begin{aligned} \rho_1^* &= -6(c^2-b^2)/[(1+2c)(1-c^2)] \\ \rho_2^* &= 2/[(1+2c)(1-c^2)] \end{aligned} \tag{4.20}$$

is an upper bound on the ineraction curve, as shown by GHI in Fig. 6. GH is inferior to our previous result, but HI shows an improvement over HC.

Similarly, the mechanism of Fig. 7(b) leads to

$$\begin{aligned} \mathbf{e}^* &= -A(c-b)[1,(c-b)(c+2b)] \\ \boldsymbol{\rho}^*.\mathbf{e}^* &= 2c|A| \\ \rho_1^*+(c-b)(c+2b)\rho_2^* &= -2c/(c-b) \end{aligned} \tag{4.21}$$

and the upper bound

$$\begin{aligned} \rho_1^* &= -4(c^3-b^3)/(b+2c)(c-b)^2 \\ \rho_2^* &= 2b/[(b+2c)(c-b)^2] \end{aligned} \tag{4.22}$$

as shown in IJ in Fig. 6. Finally, it follows from symmetry, that $IHABJ'I'H'A'B'JI$ is an upper bound on the interaction curve.

Our purpose in preparing Fig. 6 has been to illustrate how the theorems may be used to give easily computed bounds which give a fair approximation to the interaction curve. Obviously more accurate bounds can be obtained by looking for more realistic stress profiles and mechanisms and by relating them to each other.

REFERENCES

[1] D. C. Drucker, Some implications of work hardening and ideal plasticity. *Q. appl. Math.* **7**, 411–418 (1950).
[2] P. G. Hodge, Jr. and C. K. Sun, General properties of yield-point load surfaces. *J. appl. Mech.* **35**, 107–110 (1968).
[3] W. Prager, The general theory of limit design. *Proc. 8th Int. Congr. appl. Mech.* (*Istanbul, 1952*) **2**, 65–72 (1956).
[4] H. G. Hopkins and W. Prager, The load carrying capacity of circular plates. *J. Mech. Phys. Solids* **2**, 1–13 (1953).

(*Received* 8 *July* 1969)

Абстракт—Предполагаются верхняя и нижняя предельные теоремы для кривой взаимодействия точки текучести для сцсшеш, обладающих более чем одним независимым заданным параметром нагрузки. Рассматривается задача определения фактора безопасности поверхности нагрузки для сцсшеш подверженной действию заданной силы. Теория иллюстрируются примерами для балок и круглых пластинок.